

# Power Demand and Total Harmonic Distortion Analysis for an EV Charging Station Concept Utilizing a Battery Energy Storage System

Kisuk Kim\*, Chong Suk Song\*, Gilsung Byeon\*\*, Hosung Jung\*\*\*, Hyungchul Kim\*\*\*  
and Gilsoo Jang<sup>†</sup>

**Abstract** – To verify the effectiveness of the proposed system, the changes in power demand are analyzed for an AC and DC distribution system for the existing V2G concept and electric vehicle charging stations connected to a Battery Energy Storage System. In addition, since many power-converter-based chargers are operated simultaneously in an EV charging station, the change in the system harmonics when several EV chargers are connected at a single point is analyzed through simulations.

**Keywords:** Electric vehicle, V2G, Energy storage system, Power demand, THD

## 1. Introduction

Due to issues such as fossil fuel depletion, regulations for environmental pollution, and high oil prices, industry sectors have been hastening the development of alternative energy. The automotive industry, which is one of the major causes of pollution, has focused on the development of green energy solutions, which has resulted in increased interest in electric vehicles (EVs). In December 2010, the Korean government expressed its commitment to fostering the EV industry by announcing the “Green Car Development Roadmap,” and has planned to accelerate the supply by the mass production of various EVs ranging from small cars to buses by 2015 [1]. However, despite many technological advances, the proliferation of electric vehicles is being hindered by several issues, such as short driving distance, long recharging time, lack of charging and infrastructure. In order to accommodate electric vehicles, the most urgent task is the deployment of charging infrastructure, without which it is difficult to expect the market formation and diffusion of EVs.

The Smart Grid V2G concept involves the utilization of the battery power of EVs by the grid during peak hours and the charging of the batteries when the power demand is low [2]. However, this concept does not consider convenience for EVs as a means of transportation. With the V2G concept, cars may not be available when use is urgent during daytime peak hours if the power in the EV battery is being consumed during this process. Therefore, it is

necessary to reestablish a new concept that preferentially considers these factors. Existing automobile service stations comprise an underground oil tank that stores fuel to be supplied. In the same way, it is necessary to install a Battery Energy Storage System (BESS) in the basement of EV charging stations, where the electric energy is stored during low peak power, and charges EVs and supplies power to the grid during peak hours [3, 4]. When this concept is utilized, it is more feasible to secure space for the BESS installation, and it is expected that the use of EVs can be facilitated.

A method that utilizes the existing gas station concept with an energy storage device and the existing V2G EV charging scheme is compared for changes in the power demand using AC and DC distribution systems. The harmonic impact on the system when several EV chargers are connected is analyzed through simulations.

## 2. Harmonics

### 2.1 Harmonics

In general, harmonics refers to a frequency higher than the power frequency with a value of several hundred Hz, and is a periodic complex waveform other than that of the fundamental component, where the  $n$ th harmonic is defined as the frequency  $n$  times that of the primary wave. The distorted waveforms can be decomposed into one fundamental waveform and several waveforms with frequencies that are an integer multiple of the fundamental frequency. These distorted waveforms generally contain an infinite number of waves, and the frequency range that is being considered for analysis is up to the 50th harmonics (about 3 kHz), while the frequency above this range is distinguished as noise [5].

<sup>†</sup> Corresponding Author: School of Electrical Engineering, Korea University, Korea. (gjang@korea.ac.kr)

\* School of Electrical Engineering, Korea University, Korea. (kks1213, chong\_suk@korea.ac.kr)

\*\* Korea Electrotechnology Research Institute (KERI), Korea. (gsbyeon@keri.re.kr)

\*\*\* Korea Railroad Research Institute (KRRRI), Korea. ({hsjung, hckim}@krrri.re.kr)

Received: May 27, 2013; Accepted: June 7, 2013

In order to charge an EV battery, a DC supply is required. A charging system is connected to the power system through an AC/DC power converter device. The harmonics in the power conversion device are produced by a square wave that is being fed into the system during the DC/AC conversion process. When the harmonics produced exceed a permissible value in the adjacent residential loads and the system, there is a negative impact on the power quality regarding transformer output reduction, overheating of the generators or cables, power factor degradation, etc. [6]

### 2.2 Harmonics distortion degree

The Total Harmonic Distortion (THD) is an index that is most frequently used to represent the degree of wave distortion. THD, shown in Eq. (1), is the sum of the ratio of the rms value of each individual harmonic wave and the fundamental wave, and it is used to indicate the degree of harmonic generation. The two types of THD are the voltage and current THD. The former is utilized in the “KEPCO Power Supply Terms.”

$$THD = \sqrt{\sum_{h=2}^N \left(\frac{Individual(h)}{Individual(1)}\right)^2} \quad (1)$$

Table 1 shows the regulations on harmonic voltage distortion limit established by the IEEE. Table 2 present the limit of harmonic current distortion. In addition, the even harmonics are limited to 25% of the odd harmonics [7].

**Table 1.** Limits of harmonic voltage distortion

| Bus Voltage at PCC | Individual Voltage Distortion (%) | Total Voltage Distortion THD(%) |
|--------------------|-----------------------------------|---------------------------------|
| 69kV and below     | 3.0                               | 5.0                             |
| 69kV through 161kV | 1.5                               | 2.5                             |
| 161kV and above    | 1.0                               | 1.5                             |

**Table 2.** Limits of harmonic current distortion

| Isc/IL   | h<11 | 11≤h<17 | 17≤h<23 | 23≤h<35 | 35<h | TDD  |
|----------|------|---------|---------|---------|------|------|
| < 20     | 4.0  | 2.0     | 1.5     | 0.6     | 0.3  | 5.0  |
| 20~50    | 7.0  | 3.5     | 2.5     | 1.0     | 0.5  | 8.0  |
| 50~100   | 10.0 | 4.5     | 4.0     | 1.5     | 0.7  | 12.0 |
| 100~1000 | 12.0 | 5.5     | 5.0     | 2.0     | 1.0  | 15.0 |
| > 1000   | 15.0 | 7.0     | 6.0     | 2.5     | 1.4  | 20.0 |

The harmonic current injection limits for harmonic levels at the PCC(Point of Common Coupling) have been proposed for end users in the IEEE Standard 519-1992. In addition, from the supplier’s perspective, the voltage distortion at the PCC is restricted. Therefore, the end users and equipment are responsible for the harmonic current inflow and harmonic voltage harmonic distortion at the PCC.

## 3. Construction of EV Charging Station

### 3.1 Vehicle-to-Grid

V2G is one of the existing applications of Smart Grids and involves bidirectional connection of the grid and EV batteries to enable mutual power transfer. V2G is an operational measure that is based on real-time electricity prices [8]. However, the concept of V2G is not appropriate when considering the vehicle's original function as a convenient means of transportation. A vehicle has to be able to move regardless of time and place and must be able to charge immediately for low SOC levels. Therefore, for the seamless utilization of EVs, the construction of EV charging stations similar to existing gas stations is proposed in this paper.

### 3.2 EV charging station linked with BESS

The proposed EV charging station involves converting the traditional gas station concept into a form suitable for EVs. As shown in Fig. 1, there is an average of 4-6 lubricators in existing gas stations, which are supplied by a fuel tank in the underground space of the gas station. In an EV charging station, the lubricators can be replaced by chargers, and the space required for the fuel tank can be utilized for installing an energy storage device thereby negating the need for any additional space. A charging station that utilizes energy storage would be able to maintain charging capabilities during peak hours. When there is a lack of power in the system, instead of using the EV battery power to supply power to the grid, the energy stored in the energy storage device can be utilized. The energy storage device is connected in parallel with the charger and system, and has the advantage of supplying power flexibly by direct connection of the charger to the grid, connection of the charger to the energy storage device, or the connection of the energy storage device with the grid through On/Off switching functions.

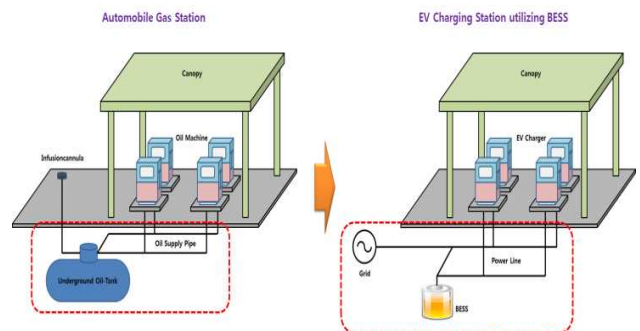


**Fig. 1.** Existing gas station infrastructure of EV charging stations

## 4. Design of Fast DC Electrical Vehicle Charger

### 4.1 EV charger configuration

EV chargers comprise AC and DC chargers. The AC chargers provide power to the EVs by utilizing the existing 220V or 380V power supplies by converting AC power to a DC form. The DC chargers provide power to the EVs by utilizing the DC distribution network voltage level of 400V as the input, and converting the DC voltage to an appropriate level for EV charging through a DC-DC converter. Figs. 2 and 3 briefly present the structure of the AC and DC charger, respectively. The DC charger is more compact and lighter than its AC counterpart, since the DC-DC converter is only required for the conversion process. In addition, since there is one less power conversion phase, the power efficiency can be improved by 3%. In this paper, the DC-type charger has been utilized to establish an EV charging station in a DC Micro Grid.

### 4.2 Charger model

Since the DC-DC converters in fast chargers normally utilize high voltage, isolated converters are normally used. However, in converters, the switching losses increase with the increase in the switching frequency, and reduce the system efficiency. Snubbers or protection circuits utilized to reduce switching losses incur additional manufacturing cost. The phase-shift full-bridge converter, which has the same structure as existing DC/DC converters, has an advantage of simple structure and feasibility in control, since soft-switching is enabled by adjusting the phase of

the lead-lag switching signal. The phase-shift full-bridge converter has the structure shown in Fig. 4, where two pairs of switches perform ON/OFF operation simultaneously. When both the switches are OFF, the load current is circulated through a diode rectifier, and a parasitic resonance phenomenon occurs between the transformer leakage inductance and the parasitic output capacitance of the switching device. The phase-shift full-bridge converter used to reduce the effect due to this parasitic resonance performs controls one of the switches to always be ON when the secondary voltage of the transformer is 0, by delaying the phase in order to secure a stable zero voltage switching (ZVS) operating area. This provides a path to circulate the current due to the leakage inductance to solve the problem of parasitic resonance between the transformer's leakage inductance and the switching device's output capacitance, such that a separate snubber circuit is not required. A high-efficiency converter can be configured due to the reduction of the switching losses and stress of the devices.

The ZVS method minimizes the Turn-On losses during switching, and the zero current switching (ZCS) method minimizes the Turn-Off losses. ZVS during OFF and ZCS during ON have the same switching losses as hard switching, so there is no significant difference in terms of loss. However, as the system capacity becomes larger, since the switching losses increase proportionally to the size of the voltage and current applied to the semiconductor switch, the improvements in the efficiency depend on whether the Turn-On loss or Turn-Off loss is minimized. In MOSFETs and IGBTs, which are utilized as switches in switching power supplies, where the Turn-On loss is generally greater than that of the Turn-Off loss. As such, it is preferable to employ the ZVS method [9]. Also, in the transformer secondary side, the transformer and diode current burden can be reduced through a Current Doubler rectification circuit, which has the advantage of reducing the output voltage and current ripple. In this paper, a DC-DC converter with phase-shift full-bridge topology has been selected.

The existing AC fast chargers comprise a 50-kW capacity and voltage of AC 220/380V, with a current of AC 110A. These chargers are designed with an efficiency of over 90%. DC fast chargers must also have a similar level

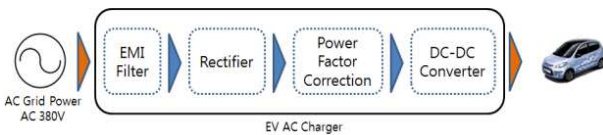


Fig. 2. Configuration of EV AC Charger

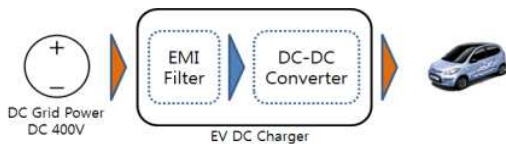


Fig. 3. Configuration of EV DC Charger

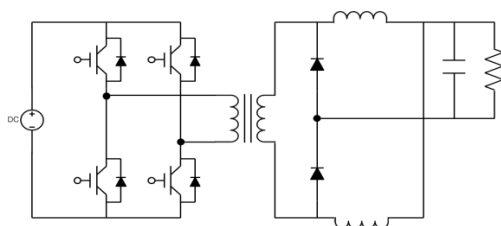


Fig. 4. Phase Shifted Full-Bridge Converter

Table 3. Fast charging system design specifications

| Item   |              | AC Charging Facility | DC Charging Facility |
|--------|--------------|----------------------|----------------------|
| Input  | Voltage      | AC 380 [V]           | DC 400 [V]           |
|        | Current      | < 110 [A]            | < 125 [A]            |
|        | Power Factor | > 0.9                | > 0.9                |
| Output | Power        | 50 [kW]              | 50 [kW]              |
|        | Voltage      | DC 450 [V]           | DC 450 [V]           |
|        | Current      | DC 110 [A]           | DC 110 [A]           |
|        | Efficiency   | > 90 [%]             | > 90 [%]             |

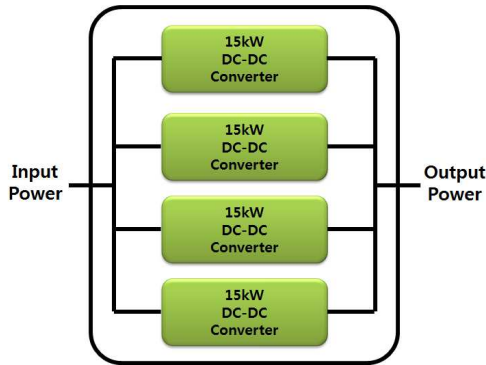


Fig. 5. Fast charger capacity design

of design specifications, and must be designed based on the DC Micro Grid distribution voltage. Table 3 shows the design specifications of the AC and DC fast charging system.

A charger has been designed according to the design specifications shown in Table 3. A 50-kW DC fast charger has been designed by modularizing two DC-DC converters and utilizing 2 of these modules, as shown in Fig. 5.

It has been verified that the designed EV charger has input/output efficiency, output voltage, and current values similar to the designed values. An EV charging model for a 50-kW Full-load reveals that the AC charger output voltage fluctuation range is from 437~458V and the output current fluctuation range is from 107~112A. For the EV DC Charger, the output voltage and current fluctuation range are 447~452V and 101~112A, respectively. The efficiencies of the EVAC Charger and DC Charger are 91.27% and 94.84%, respectively. The DC charger, which has fewer power conversion stages, was found to have efficiency improved by 3.57% through simulations.

### 4.3 Battery model

The EV battery was simulated using a lithium-ion polymer battery model, with a distance traveled per charge of 140km, 16.4-kWh capacity, 360V battery voltage, and a rapid charging time of approximately 25minutes.

The capacity of the energy storage device is 100kWh and the battery voltage is modeled with the same voltage level of the 400V DC distribution system.

Various Lithium-ion polymer battery equivalent models exist for battery modeling. Instead of utilizing a complex battery model, the lithium-ion polymer battery is represented by a resistor-capacitor series circuit, as shown in Fig. 6 [10, 11]. The initial voltage of  $C_b$  in the equivalent model is 0, and  $V_b$ , which is the capacitor's theoretical initial voltage is the initial value of the lithium-ion charging/discharging system. The capacitor  $C_b$  in the Lithium-ion polymer battery equivalent model can be extracted from the formula  $Q=CV$ .

In order to determine  $R_b$  of the lithium-ion polymer battery model, the time constant values are determined by

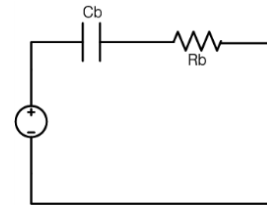


Fig. 6. Battery equivalent model

performing charging tests of an actual Lithium-ion polymer battery. However, since this study is to investigate the brief trends, simulations are performed by applying the generalized resistance value of 50mΩ.

## 5. DC Microgrid Configuration

Fig. 7 presents the distribution system diagram for each simulation case. The 154kV transmission system is modeled as an infinite bus system, and the power is supplied to the distribution system through a 154/22.9-kV main transformer. The 22.9-kV line utilizes a 3-km AWOC 160 AL95 high-voltage line, and the 380V line uses a 500-m OW60 low-voltage line. Table 4 shows the main parameters of the distribution system.

The distribution system is configured with a total of 4 feeders. The AC distribution system comprises feeders #1, #2, and #4, and the DC distribution system contains feeder #3. The DC distribution system utilizes a 400Vdc voltage, which is presently being considered in South Korea. The low-voltage residential load is configured as follows: feeders #1 and #4 have loads of 2.20MW and 3.65MW, respectively, and feeders #2 and #3 have loads that vary on an hourly basis.

Each case has been configured as shown in Fig. 9. In

Table 4. Type sizes for camera-ready papers

| Classification          | Facility          | Parameter  |  |
|-------------------------|-------------------|--|--|
| Distribution Substation | Parent System     | <ul style="list-style-type: none"> <li>• 100MVA, 154/22.9kV</li> <li>• Y-Y-Δ</li> <li>• Direct Grounding type</li> </ul> |  |
|                         | Main Transformer  | <ul style="list-style-type: none"> <li>• 45MVA</li> <li>• Y-Y</li> </ul>   |  |
| Distribution Line       | Power Source      | <ul style="list-style-type: none"> <li>• 22.9kV High Voltage</li> <li>• 380Vac, 400Vdc</li> </ul>                        |  |
|                         | Distribution Line | <ul style="list-style-type: none"> <li>• AWOC 160 AL95(22.9kV)</li> <li>• OW60 WO60 (380V)</li> </ul>                    |  |
|                         | Residential Load  | Feeder #1  | <ul style="list-style-type: none"> <li>• AC Load</li> <li>• 2.20MW / 1.05Var</li> </ul>                              |
|                         |                   | Feeder #2  | <ul style="list-style-type: none"> <li>• AC Load</li> <li>• EV AC Charging Station</li> <li>• BESS 100kWh</li> </ul> |
|                         |                   | Feeder #3  | <ul style="list-style-type: none"> <li>• DC Load</li> <li>• EV DC Charging Station</li> <li>• BESS 100kWh</li> </ul> |
| Feeder #4               |                   | <ul style="list-style-type: none"> <li>• AC Load</li> <li>• 3.65MW / 1.02Var</li> </ul>                                  |  |

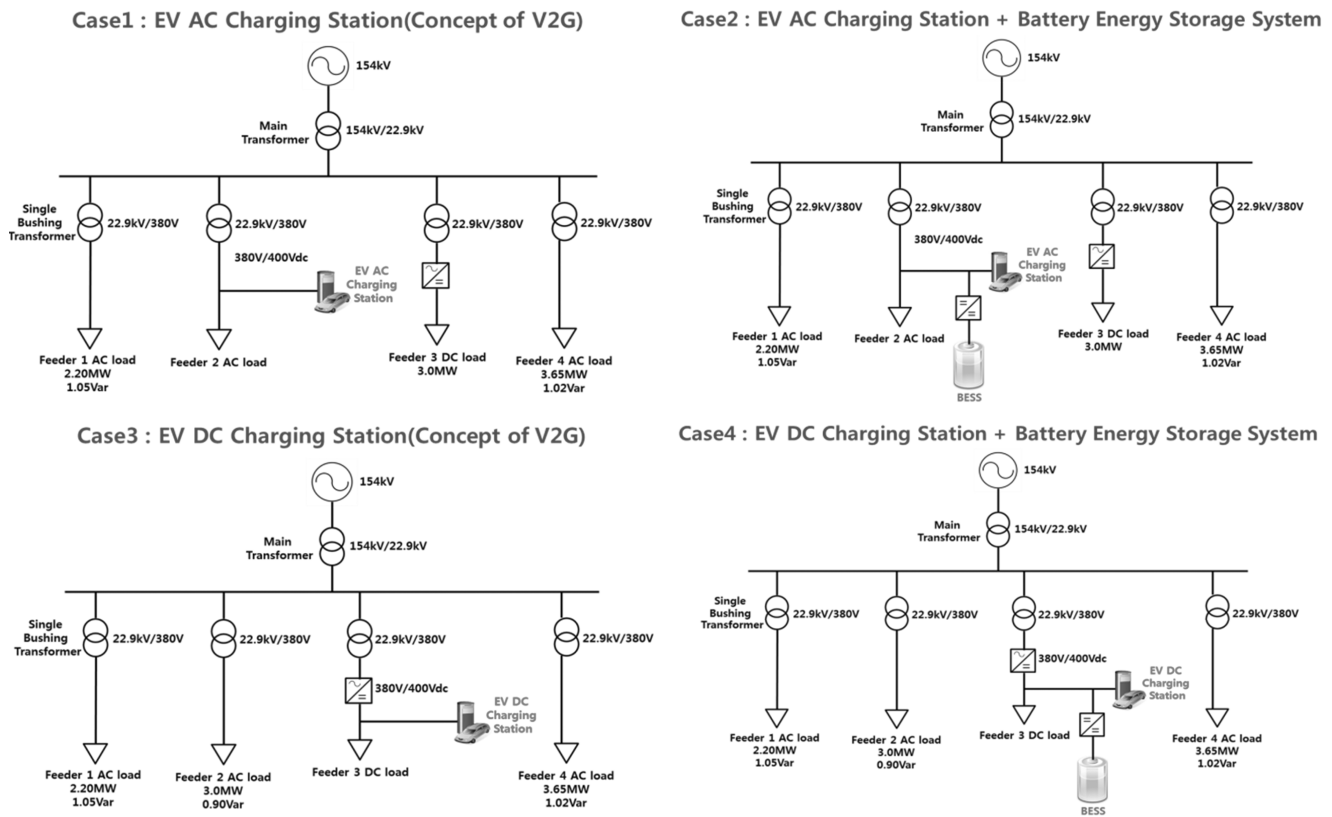


Fig. 7. Case-specific distribution system configuration

Table 5. Number of devices used on an hourly basis

| Classification | TV   | Washer | A/C | Electric Iron | Computer | Electric Cooker | Microwave | Vacuum Cleaner | Hair Dryer | Audio |
|----------------|------|--------|-----|---------------|----------|-----------------|-----------|----------------|------------|-------|
| 00-01          | 963  | 12     | 36  | 1             | 365      | 646             | 1         | 2              | 9          | 4     |
| 01-02          | 187  | 3      | 18  | -             | 150      | 625             | -         | -              | 2          | -     |
| 02-03          | 66   | 3      | 5   | 1             | 52       | 616             | -         | -              | -          | -     |
| 03-04          | 16   | 2      | 4   | 1             | 17       | 613             | -         | -              | 1          | -     |
| 04-05          | 5    | 2      | 3   | -             | 17       | 609             | -         | 1              | -          | -     |
| 05-06          | 33   | 21     | 9   | 5             | 26       | 660             | 2         | 29             | 16         | 11    |
| 06-07          | 352  | 103    | 5   | 10            | 41       | 978             | 66        | 44             | 248        | 8     |
| 07-08          | 942  | 413    | 5   | 78            | 89       | 1510            | 265       | 216            | 850        | 17    |
| 08-09          | 1224 | 609    | 4   | 88            | 127      | 1413            | 280       | 368            | 752        | 47    |
| 09-10          | 1105 | 458    | 11  | 118           | 174      | 1126            | 82        | 374            | 302        | 30    |
| 10-11          | 759  | 285    | 24  | 119           | 233      | 1067            | 47        | 233            | 97         | 22    |
| 11-12          | 519  | 159    | 40  | 80            | 265      | 1052            | 35        | 12.2           | 67         | 30    |
| 12-13          | 360  | 99     | 63  | 49            | 263      | 1064            | 83        | 87             | 41         | 49    |
| 13-14          | 329  | 111    | 84  | 37            | 342      | 1028            | 108       | 92             | 26         | 38    |
| 14-15          | 363  | 99     | 85  | 25            | 397      | 942             | 46        | 65             | 21         | 38    |
| 15-16          | 458  | 80     | 61  | 30            | 462      | 923             | 31        | 43             | 16         | 32    |
| 16-17          | 578  | 86     | 47  | 38            | 508      | 934             | 31        | 83             | 21         | 31    |
| 17-18          | 890  | 119    | 50  | 43            | 654      | 1025            | 69        | 142            | 23         | 43    |
| 18-19          | 1447 | 186    | 73  | 72            | 866      | 1195            | 139       | 206            | 41         | 54    |
| 19-20          | 2100 | 208    | 98  | 68            | 1155     | 1100            | 160       | 186            | 45         | 61    |
| 20-21          | 2679 | 186    | 125 | 60            | 1371     | 956             | 122       | 92             | 37         | 56    |
| 21-22          | 2897 | 134    | 123 | 55            | 1297     | 789             | 48        | 61             | 30         | 39    |
| 22-23          | 2675 | 97     | 90  | 20            | 1071     | 713             | 17        | 28             | 27         | 35    |
| 23-24          | 1985 | 50     | 77  | 4             | 729      | 672             | 8         | 5              | 13         | 19    |



Case 1, the EV AC Charging Station has been connected to feeder #2, whereas in Case 2, the EV AC Charging Station and BESS are connected to feeder #2 in parallel. In Cases 3 and 4, the EV DC Charging Station and BESS are connected to feeder #3, similar to Cases 1 and 2 [12, 13]. The EV Charging Station is configured with 6 chargers for both the AC and DC type.

### 6. Simulations

MATLAB/Simulink has been used to perform simulations for the EV charging station connected to a BESS. Fig. 8 shows a schematic diagram of the simulation. The simulations have been performed to analyze the load demand pattern and harmonic impacts.

#### 6.1. Load demand patterns analysis

In order to analyze the load demand pattern, the data from KPX's '2009 Survey on Penetration of Consumer

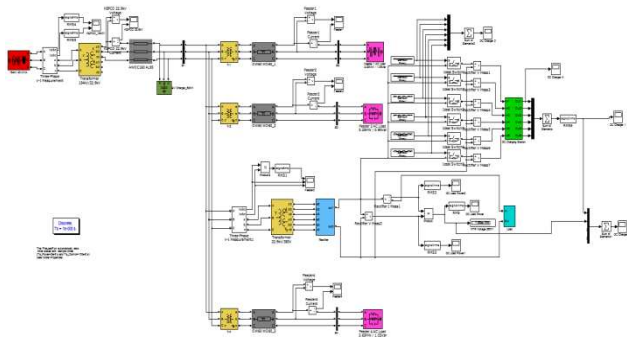


Fig. 8. MATLAB/Simulink Simulation

Table 6. Power consumption of each device

|                |                 |           |                |               |          |
|----------------|-----------------|-----------|----------------|---------------|----------|
| Classification | TV              | Washer    | A/C            | Electric Iron | Computer |
| Power [W]      | 149.1           | 506.5     | 953.4          | 1233.8        | 153.0    |
| Classification | Electric Cooker | Microwave | Vacuum Cleaner | Hair Dryer    | Audio    |
| Power [W]      | 567.8           | 1065.9    | 1075.3         | 57            | 37.5     |

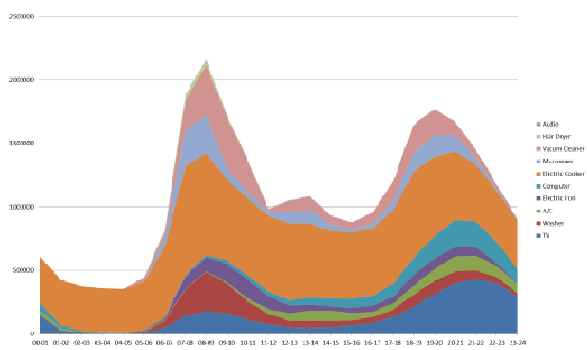


Fig. 9. Hourly household power equipment load pattern

Appliances and Household Electricity Consumption Behavior' has been utilized. Table 5 provides the number of devices used on an hourly basis, and Table 6 shows the power consumption of each device. The setables have been applied to compose the hourly load pattern [14]. Fig. 9 shows the hourly household power equipment load pattern.

A random function is used for generating the hourly number of operating EV chargers. The number of operating chargers for each hour is being enlisted in Table. 7.

Fig. 10 shows the loads for the cases when the EV charging infrastructure is connected to the AC distribution system, when the V2G concept is applied, and when the BESS is considered. During peak loads, the power consumption reduction is the greatest when the V2G concept is applied. For the case with the BESS, the power consumption is reduced to a certain extent, even though the change is smaller compared to the case with V2G. In this paper, the capacity of the BESS has been selected as 100kWh to fit the load of the EV charging station, and since the capacity is small compared to the total load of the distribution system, it has been observed that the reduction in peak power is comparatively lower than that in the V2G case. However, in the case with V2G, when the total load is smaller, the total charging amount is increased, but in the case when the BESS is applied, the change is smaller than that with the V2G, which makes it more effective. Fig. 11 shows the loads when the EV charging system is connected to the DC distribution system, when the V2G concept is applied, and when the BESS is applied. Results similar to those of the AC distribution system are obtained.

Fig. 12 shows the graph for the load according to the hourly operating EV charger count for the AC and DC

Table 7. Hourly number of operating EV chargers

|        |       |       |       |       |       |       |
|--------|-------|-------|-------|-------|-------|-------|
| Time   | 00-01 | 01-02 | 02-03 | 03-04 | 04-05 | 05-06 |
| Number | 5     | 4     | 3     | 4     | 2     | 4     |
| Time   | 06-07 | 07-08 | 08-09 | 09-10 | 10-11 | 11-12 |
| Number | 6     | 2     | 3     | 4     | 3     | 4     |
| Time   | 12-13 | 13-14 | 14-15 | 15-16 | 16-17 | 17-18 |
| Number | 2     | 3     | 3     | 4     | 2     | 1     |
| Time   | 18-19 | 19-20 | 20-21 | 21-22 | 22-23 | 23-24 |
| Number | 2     | 1     | 6     | 3     | 3     | 3     |

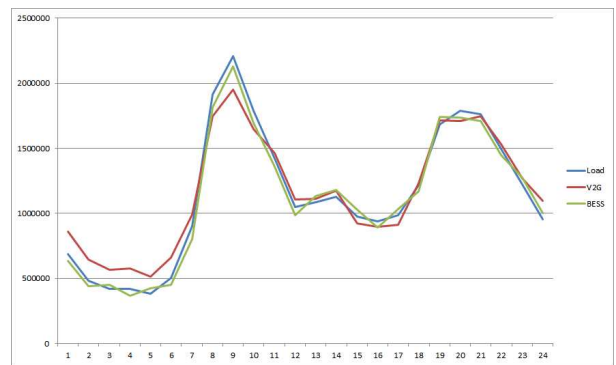


Fig. 10. Demand load pattern for AC connection

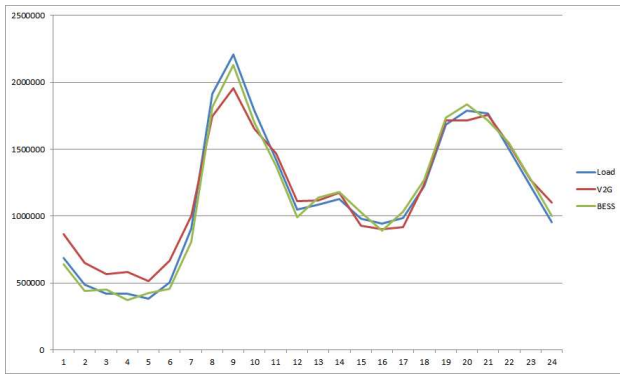


Fig. 11. Demand load pattern for DC connection

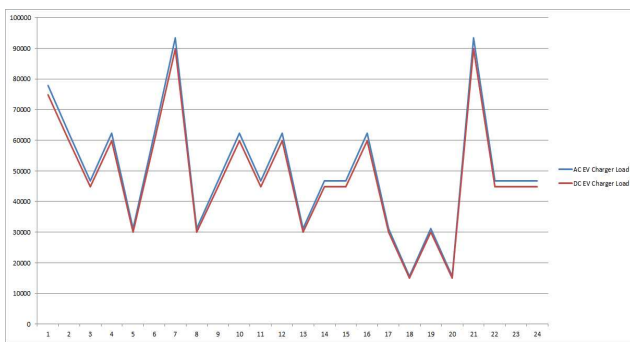


Fig. 12. Hourly EV charger demand load pattern

methods, respectively. The reason why the EV DC charger consumes lesser energy than the EV AC Charger is because the EV DC Charger’s efficiency is 3% better than the AC counterpart, resulting in less energy consumption for the same amount of load.

### 6.2 Harmonic effect analysis

In order to analyze the impact of the DC Micro Grid on the system, MATLAB/Simulink has been used for simulation, along with FFT Analysis. Table 8 shows the results for the harmonic analysis at the 22.9V line PCC when the EV Station is not connected, when the EV station is connected to the DC distribution system, and when the EV station and BESS are connected to the DC distribution system. It has been confirmed that the THD value is within the specified ranges for all of these cases. When only the EV Station is linked, the charge in the voltage THD is negligible, but compared with the case when the EV Station is not connected for the case of current THD, a twofold increase is observed. In the case when the EV Station and BESS are connected, the voltage and current THD are increased by twofold and 30 percent, respectively, compared with the case when the EV Station is not connected. This is because the addition of power conversion devices results in an increase in the harmonics, and in the case when the EV Station and BESS are connected, the harmonics of each power conversion device

Table 8. Harmonics of each type

|     | No EV Station |         | EV Station |         | EV Station+BESS |         |
|-----|---------------|---------|------------|---------|-----------------|---------|
|     | Voltage       | Current | Voltage    | Current | Voltage         | Current |
| THD | 0.09          | 0.07    | 0.10       | 0.15    | 0.18            | 0.10    |
| 1   | 100           | 100     | 100        | 100     | 100             | 100     |
| 3   | 0             | 0       | 0          | 0.07    | 0               | 0.01    |
| 5   | 0.01          | 0.06    | 0.01       | 0.05    | 0.01            | 0.06    |
| 7   | 0.01          | 0.03    | 0.01       | 0.02    | 0.02            | 0.05    |
| 9   | 0             | 0       | 0.02       | 0       | 0               | 0.01    |
| 11  | 0.03          | 0.02    | 0.03       | 0.01    | 0.04            | 0.03    |
| 13  | 0.08          | 0       | 0.03       | 0.02    | 0.17            | 0.01    |
| 15  | 0             | 0       | 0.03       | 0.01    | 0.01            | 0       |
| 17  | 0.02          | 0.02    | 0.01       | 0.01    | 0.02            | 0.03    |
| 19  | 0.01          | 0.01    | 0.01       | 0       | 0.01            | 0.02    |
| 21  | 0             | 0       | 0.01       | 0.01    | 0               | 0       |
| 23  | 0             | 0.01    | 0          | 0.01    | 0               | 0       |
| 25  | 0             | 0.01    | 0          | 0.01    | 0               | 0       |

Table 9. Residential load harmonics(EV Station + BESS)

|     | Feeder 1 |         | Feeder 2 |         | Feeder 3 |         | Feeder 4 |         |
|-----|----------|---------|----------|---------|----------|---------|----------|---------|
|     | Voltage  | Current | Voltage  | Current | Voltage  | Current | Voltage  | Current |
| THD | 0.05     | 0.05    | 0.04     | 0.04    | 0.19     | 2.13    | 0.04     | 0.04    |
| 1   | 100      | 100     | 100      | 100     | 100      | 100     | 100      | 100     |
| 3   | 0        | 0       | 0        | 0       | 0        | 0.02    | 0        | 0       |
| 5   | 0.01     | 0.01    | 0.01     | 0       | 0.02     | 0.08    | 0.01     | 0       |
| 7   | 0.01     | 0.01    | 0.01     | 0.01    | 0.02     | 0.17    | 0.01     | 0.01    |
| 9   | 0        | 0       | 0        | 0       | 0        | 0.06    | 0        | 0       |
| 11  | 0.01     | 0.01    | 0.01     | 0.01    | 0.05     | 0.52    | 0.01     | 0.01    |
| 13  | 0.05     | 0.05    | 0.04     | 0.04    | 0.18     | 2.02    | 0.03     | 0.03    |
| 15  | 0        | 0       | 0        | 0       | 0.01     | 0.11    | 0        | 0       |
| 17  | 0        | 0       | 0        | 0       | 0.01     | 0.22    | 0        | 0       |
| 19  | 0        | 0       | 0        | 0       | 0        | 0.10    | 0        | 0       |
| 21  | 0        | 0       | 0        | 0       | 0        | 0.02    | 0        | 0       |
| 23  | 0        | 0       | 0        | 0       | 0        | 0       | 0        | 0       |
| 25  | 0        | 0       | 0        | 0       | 0        | 0.01    | 0        | 0       |

cancel each other out, resulting in a slightly lower increase in the current THD.

The harmonics of each feeder has been examined when the EV Station and BESS are connected, and the results are shown in Table 9. Feeders #1, #2, and #4, which are AC loads, all have values that fall within the normal ranges. In the case of the low-voltage DC distribution system (Feeder #3), the values are within the specified ranges, but the current THD is found to be comparatively larger than that in the other feeders. It is also observed that the 13<sup>th</sup> harmonic component, which is 2.02%, is much higher compared to the other harmonic orders. This is due to the fact that the EV station, BESS, and DC loads, which include power conversion devices, are concentrated in Feeder #3, so such an effect is expected. Therefore, when configuring a DC Micro Grid, in order to

**Table 10.** Transmission system harmonics (EV Station + BESS)

|     | Primary Side of M.Tr. |                   | Secondary Side of M.Tr. |                   |
|-----|-----------------------|-------------------|-------------------------|-------------------|
|     | Voltage Harmonics     | Current Harmonics | Voltage Harmonics       | Current Harmonics |
| THD | 0.01                  | 0.40              | 0.11                    | 0.40              |
| 1   | 100                   | 100               | 100                     | 100               |
| 3   | 0                     | 0.01              | 0                       | 0.01              |
| 5   | 0                     | 0.07              | 0.01                    | 0.07              |
| 7   | 0                     | 0.08              | 0.01                    | 0.08              |
| 9   | 0                     | 0.01              | 0                       | 0.01              |
| 11  | 0                     | 0.11              | 0.03                    | 0.12              |
| 13  | 0.01                  | 0.36              | 0.10                    | 0.37              |
| 15  | 0                     | 0.01              | 0.01                    | 0.01              |
| 17  | 0                     | 0.03              | 0.01                    | 0.03              |
| 19  | 0                     | 0.01              | 0.01                    | 0.01              |
| 21  | 0                     | 0                 | 0                       | 0                 |
| 23  | 0                     | 0                 | 0                       | 0                 |
| 25  | 0                     | 0                 | 0                       | 0                 |

prevent an increase in the harmonics in the grid, a harmonic filter design should also be considered.

Table 10 shows the harmonics across the 154-kV/22.9-kV transformer when the EV charging station and the BESS are connected to the DC Micro Grid. A slight increase has been observed for the current harmonics due to the influence of feeder #3, but it is within the specified range, and has minimal effect on the transmission grid. However, since only 6 EV chargers have been implemented in the EV charging station and 100kW BESS has been applied, if the number of EV chargers and capacity of BESS increases, the effect on the parent system would increase.

## 7. Conclusion

In this paper, a novel approach for utilizing the V2G concept has been proposed, and the changes in the demand load and the harmonic issues in the power system, when an EV charging system with a BESS is connected to the system have been analyzed using MATLAB/Simulink simulations.

The utilization of EV batteries to provide power during peak periods utilizing the concept of V2G is not appropriate for the automobile industry since it negatively affects user convenience. Therefore, for user-centric EV operation and the reduction of system peak power, an EV charging system approach utilizing the existing gas station method by connecting a BESS is proposed. By analyzing the demand load pattern by comparing the method of an EV charging station connecting a BESS with the V2G concept, it has been observed that the peak power reduction is more effective for the V2G concept. However, the

capacity of the BESS has been set to 100kWh, which is relatively small compared to the total load, making it less effective. Therefore, when the capacity of the BESS is set considering the total load and installing several EV charging stations in the distribution system, the effect of the BESS is expected to increase to a certain degree.

In addition, for the harmonic effect on the system when the BESS is connected to the EV charging station in a DC Micro Grid, it has been confirmed that the harmonics increase due to the increase in the number of power converting devices. It has been observed that for current harmonics, although within the specified ranges, the value increased slightly for 6 EV chargers and one 100-kW BESS connected to the grid. This shows that the subsequent increase in the number of EV chargers and capacity of BESS would increase the power quality impact on the transmission system. For future works, research is required for a more effective interconnection of the EV charging station with a BESS within a DC Micro Grid.

## Acknowledgements

This work was supported by the Human Resources Development program (No. 20114010203010) of the Korea Institute of Energy Technology Evaluation and Planning (KETEP) grant funded by the Korea government Ministry of Trade, Industry and Energy.

## References

- [1] Ministry of Knowledge Economy, "Green Car industry development strategies and challenges", 2010
- [2] S. B. Peterson, J. F. Whitacre, and J. Apt, "The economics of using plug-in hybrid electric vehicle battery packs for grid storage," *J. Power Sources*, vol. 195, no. 8, pp. 2377-2384, Apr. 2010.
- [3] XIE, Wei-dong, LUAN, Wei, "Modeling and Simulation of Public EV Charging Station with Power Storage System", *2011 International Conference on Electric Information and Control Engineering*, pp. 346~2350, April. 2011.
- [4] Kejun Qian, Chengke Zhou, Malcolm Allan, Yue Yuan, "Modeling of Load Demand Due to EV Battery Charging in Distribution Systems", *IEEE Transactions on Power Systems*, Vol. 26, No. 2, May. 2011.
- [5] Roger C. Dugan, "Electrical Power System Quality 2nd," *McGraw-Hill*, 2003
- [6] J. Carlos Gomez, Medhat M. Morcos, "Impact of EV Battery Chargers on the Power Quality of Distribution Systems", *IEEE Transactions on Power Delivery*, Vol. 18, No. 3, pp. 975~981, July. 2003.
- [7] *IEEE Standard 519-1992*
- [8] Koichiro Shimizu, Taisuke Masuta, Yuyaka Ota,



Akihiko Yokoyama, "Load Frequency Control in Power System Using Vehicle-to-Grid System Considering the Customer Convenience of Electric Vehicles", *2010 International Conference on Power System Technology*, pp.1~8, Oct. 2010.

- [9] Jeong-Gyn Lim, Se-Kyo Chung, "Digital Control of Phase-Shifted Full-Bridge PWM Converter", *2007 7<sup>th</sup> International Conference on Power Electronics*, pp. 772~777, Oct. 2007.
- [10] TarunHuria, Massimo Ceraolo, Javier Gazzarri, Robyn Jackey, "High Fidelity Electrical Model with Thermal Dependence for Characterization and Simulation of High Power Lithium Battery Cells", *Electric Vehicle Conference, 2012 IEEE International*, March. 2012.
- [11] Pavol Bauer, Neil Stenbridge, Jere mie Doppler, Praveen Kumar, "Battery Modeling and Fast Charging of EV", *14<sup>th</sup> International Power Electronics and Motion Control Conference*, pp.S11-39~S11-45, 2010.
- [12] S.A. Elankurisil, S.S. Dash, "Digital simulation of closed loop control of bi-directional dc-dc converter", *International Journal of Engineering Science and Technology*, Vol. 3, No.2, pp. 1113~1123, Feb. 2011.
- [13] Premananda any, R. K. Singh, R. K. Tripathi, "Bidirectional DC-DC converter fed drive for electric vehicle system", *International Journal of Engineering, Science and Technology*, Vol. 3, No. 3, pp. 101~110, 2011.
- [14] KPX, "2009 Survey on Penetration of Consumer Appliances and Household Electricity Consumption Behavior", 2009



**Kisuk Kim** He received a B.S. degree in electrical engineering from Soongsil University, Seoul, Korea in 2010 and an M.S. degree from Korea University, Seoul, Korea in 2013. He is currently pursuing a Ph.D. degree at Korea University. His research interests are electrical railways and real-time simulation of power systems.



**Chong Suk Song** He received B.S. and M.S. degrees from Korea University, Seoul, Korea in 2008 and 2010, respectively. Currently, he is pursuing his Ph.D. degree at Korea University. His research interests include transmission and distribution system analysis, power system visualizations, and hybrid simulation of power systems.



**Gilsung Byeon** He received B.S. and Ph.D. degrees from the School of Electrical Engineering, Korea University, in 2006 and 2012. Currently, he works as a Senior Researcher at the Smart Distribution Research Center at the Korea Electrotechnology Research Institute (KERI) in Changwon, Korea.

His research interests include distribution energy resources modeling, control, and hardware in-the-loop simulations.



**Hosung Jung** He received B.S, M.S and Ph.D. degrees in electrical engineering from Sungkyunkwan University, Suwon, Korea, in 1996, 1998 and 2002. Currently, he works as a Senior Researcher in the Internodal Transfer Systems Research Team, Korea Railroad Research Institute (KRRRI), Uiwang, Korea. His research interests include rail way feeding systems and power systems.

Korea. His research interests include rail way feeding systems and power systems.



**Hyungchul Kim** He received his B.S. and M.S. degrees in Electrical Engineering from Korea University, Seoul, Korea in 1991 and 1993, respectively. He then worked for LG electronics Inc., for 6 years. He received a Ph.D. degree from Texas A&M University in August 2003, studying power system reliability

including security analysis and reliability cost in power systems. Currently, he has been working for the Korea Railroad Research Institute (KRRRI), Uiwang, Korea, since 2004. His research interests are maintenance and security in traction power systems, and energy supply for railway.



**Gilsoo Jang** He received B.S. and M.S. degrees in electrical engineering from Korea University, Seoul, Korea, in 1991 and 1994, respectively, and a Ph.D. degree in electrical and computer engineering from Iowa State University, Ames, in 1997. He was a Visiting Scientist at Iowa State University from

1997 to 1998, and a Senior Researcher with the Korea Electric Power Research Institute, Daejeon, Korea, from 1998 to 2000. Currently, he is a professor in the School of Electrical Engineering, Korea University. His research interests include power quality and power system control.